Electronic Supplementary Information

Concave Degree Engineering of One-dimensional Au-Cu Alloy Nanorods with Partial Intermetallic Compounds by Facile Wet Chemical Synthesis

Xiaoqian Gao, Zhi Wang, Yinling Zhang, Yaoyao Ren, Guan Sheng, Wei Shao, Qiaoli Chen*

College of Chemical Engineering and State Key Laboratory Breeding Base of Green Chemistry Synthesis Technology, Zhejiang University of Technology, Hangzhou, 310014, Zhejiang, China

Experimental Section

Chemical and Materials.

Tetrachoroaurate trihydrate ($HAuCl_4$, Au≥49%) and Copper(II) acetylacetonate ($Cu(acac)_2$, 99.9%) were purchased from Sigma-Aldrich. Oleylamine (OAm, 80 ~ 90%) was purchased from Shanghai Aladdin Biochemical Technology Co. Ltd. Ethanol and hexane were purchased from Sinopharm Chemical Reagent Co., Ltd.

Synthesis of concave and normal Au-Cu nanorods.

In the preparation of concave Au-Cu nanorods, 3 mL oleylamine containing 6 mg $HAuCl_4$ (the concentration of $HAuCl_4$ was 0.005 M) was heated in 140 ℃ for 20 min without any disturbance. The color of solution was changed from yellow to colorless and at last wine red, indicating the reduction of $AuCl_4^-$ to Au^+ and finally Au^0. Then 1 mL oleylamine containing 16 mg $Cu(acac)_2$ was injected into the solution and the mixture was heated in 140 ℃ for another 5 h. After the glass vial that used for wet chemical synthesis was cooled to room temperature, the products were washed with hexane/ethanol (volume ratio is 1:1) mixture and sonicated at 8800 rpm for three times and then were dissolved in ethanol for further analysis. As for the synthesis of

normal Au-Cu nanorods, the addition of $HAuCl_4$ and $Cu(acac)_2$ was double with the molar ratio of $HAuCl_4$ and $Cu(acac)_2$ keeping at 1:4 as that in the preparation of concave samples.

Structure and composition characterizations.

For transmission electron microscopic (TEM) analysis, all samples were prepared by dropping ethanol dispersion on carbon film coated copper TEM grids. Low-magnification TEM images were obtained on a Hitachi 7700 microscope operated at 120 kV. The high-angle annular dark-field scanning transmission electron microscopy (HAADF-STEM) and energy dispersive X-ray spectroscopy (EDS) were conducted with microscope operated at 300 kV. The content of Au and Cu were determined by the atom absorption spectrometry (AAS) for further used in catalytic performance. The crystal phase of the prepared samples was collected by X-ray diffraction (XRD) using a Rigaku Ultima IV X-ray diffractometer with Cu Kα radiation. X-ray photoelectron spectroscopy (XPS) analysis was taken on a K-Alpha X-ray photoelectron spectrometer (Thermo Fisher Scientific, America). All the XPS spectra have been done calibration by using the C1s that locates at 284.8 eV. The UV-vis absorption spectra were acquired on a fiber-optic spectrometer (Avalight-DH-S-BAL).

P-nitrophenol reduction reaction measurement.

The aqueous solution containing 800 μL 80 μM p-nitrophenol and freshly prepared 50 μL 0.5 M $NaBH_4$ solution were mixed thoroughly and the color of the mixture was turned into deep yellow. Then 150 μL catalyst suspension containing 200 μg Au (determined by AAS) was injected into the mixed solution. The UV-vis spectra were recorded as the reaction progress. The rate constants of this reaction were calculated according to the absorbance at 400 nm in spectra.

Electrochemical measurement.

All the electrochemical measurements were investigated on an electrochemical workstation (CHI 760E, Shanghai Chenhua Co., China) in a typical three-electrode H-cell system separated with anion exchange membrane. The Au-Cu nanorods together with 10 μL 0.5% Nafion were dissolved in ethanol to obtain catalyst suspension. Then the electrocatalysts (200 μg Au

determined by AAS) was dropped onto a carbon cloth (1 x 1 = 1 cm^2) and used as the working electrode. The Ag/AgCl electrode and the Pt electrode were used as the reference electrode and counter electrode, respectively. Before the electrochemical measurement was performed, 0.1 M $KHCO_3$ electrolyte was bubbled with CO_2 for 30 minutes. CO_2 was purged into the electrolyte continuously at 20 sccm during the electrocatalysis process. The gas products (H_2 and CO) were analyzed online by gas chromatograph (GC). The concentrations of H_2 and CO were analyzed through the thermal conductivity detector (TCD) and the flame ionization detector (FID), respectively.

Table S1. Atomic ratio of C-AuCu nanorods and N-AuCu nanorods determined by EDS and XPS.

Catalysts	EDS	XPS
C-AuCu nanorods	17%Au:83%Cu	19%Au:81%Cu
N-AuCu nanorods	14%Au:86%Cu	22%Au:78%Cu

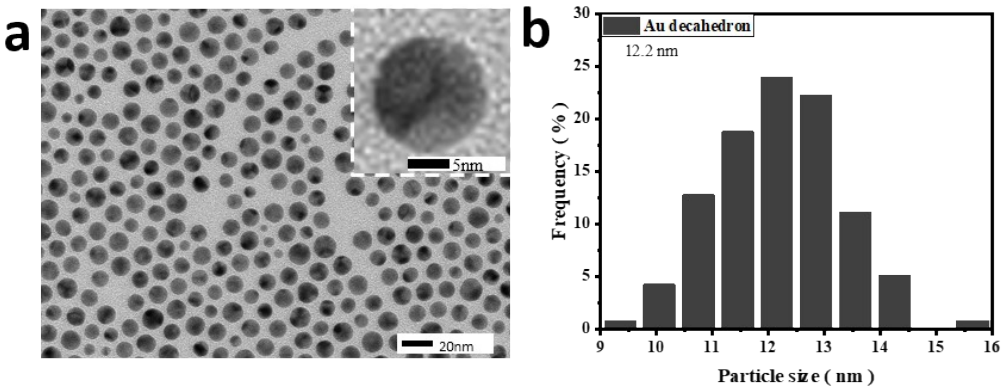

Fig. S1 (a) TEM image of Au decahedrons and (b) the corresponding particle size distribution histogram.

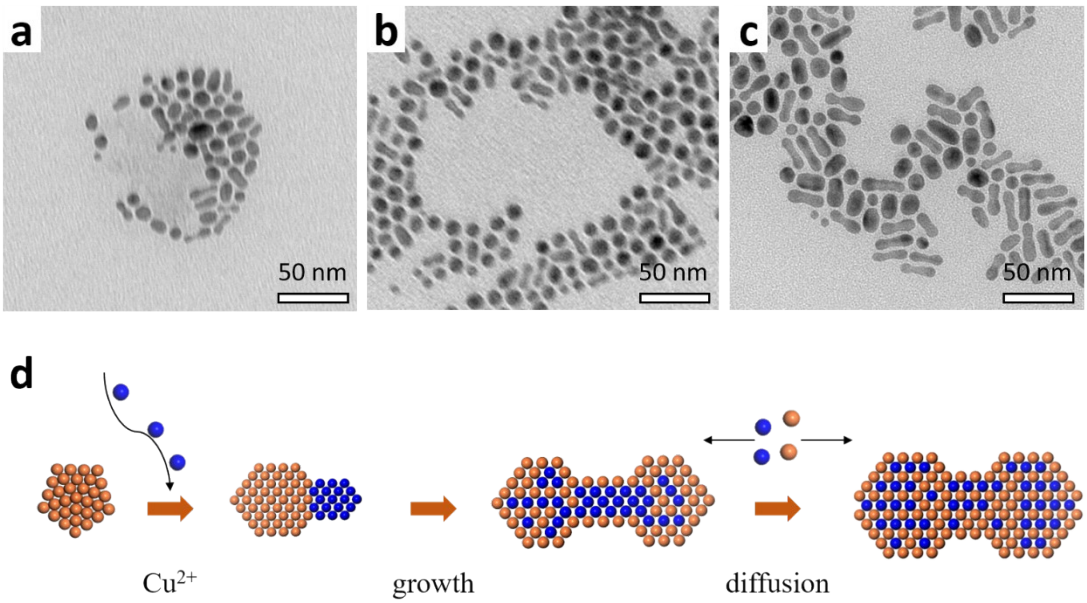

Fig. S2 TEM images of C-AuCu nanorods obtained at (a) 10 min, (b) 25 min and (c) 5 h. (d) Schematic illustration of growth mechanism for C-AuCu nanorods.

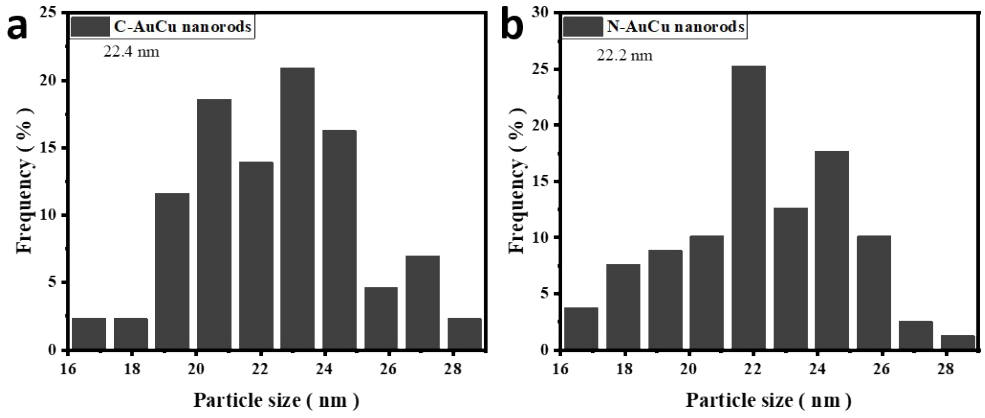

Fig. S3 Particle size distribution histograms of (a) C-AuCu nanorods and (b) N-AuCu nanorods.

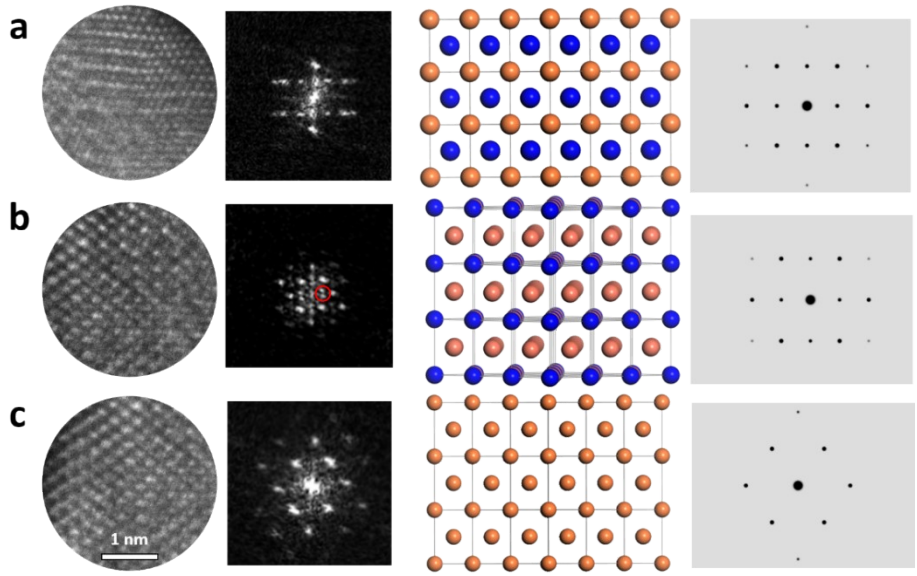

Fig. S4 Corresponding analysis of the area marked with yellow circles in Fig.2b. Enlarged HAADF-STEM images, FFT patterns, atomic models and the fitting FFT patterns of (a) intermetallic compound AuCu (the upper yellow circle), (b) intermetallic compound Cu_3Au (the middle circle) and (c) Au (the bottom circle) along the [110] direction. (To have a better comparison, HAADF-STEM images and FFT patterns are rotated by the same angle)

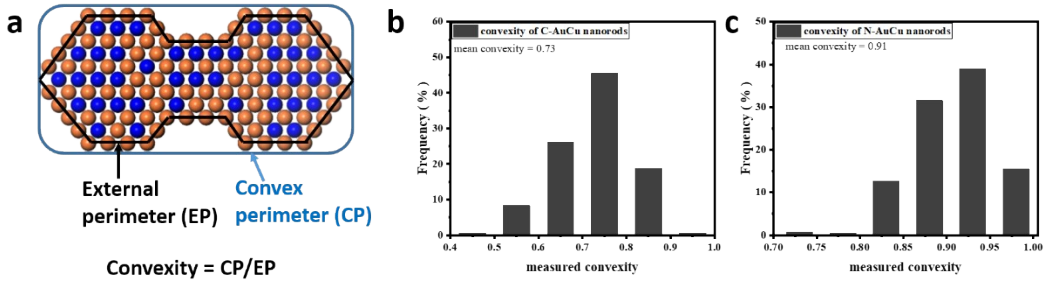

Fig. S5 (a) Schematic illustration showing the definition of convexity. Distribution of measured convexities over (b) C-AuCu nanorods and (c) N-AuCu nanorods.

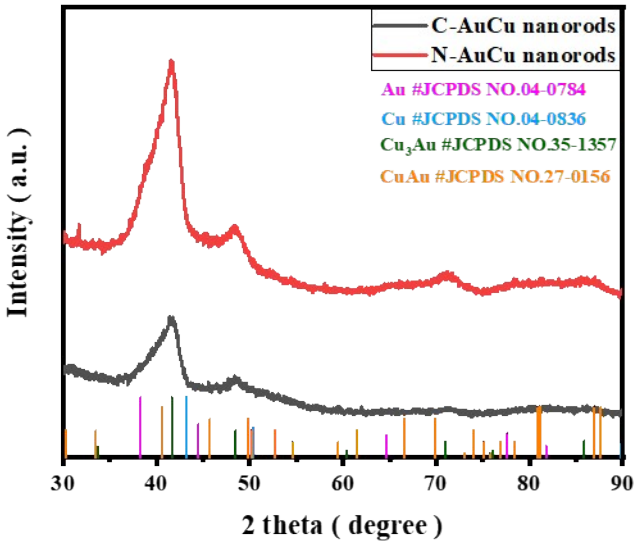

Fig. S6 XRD patterns of C-AuCu nanorods and N-AuCu nanorods.

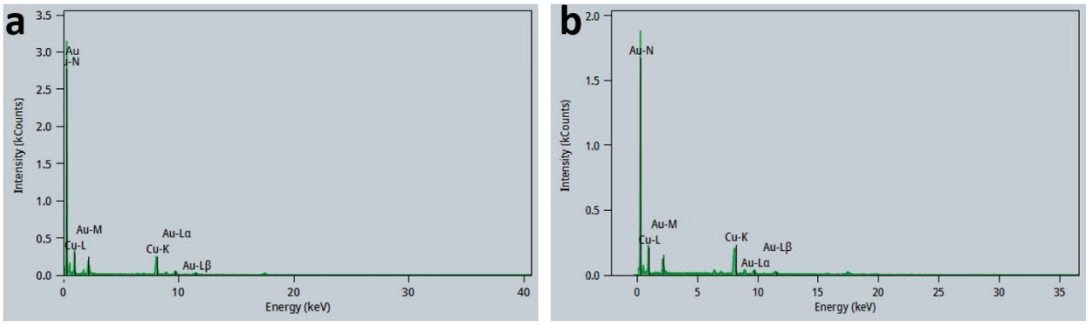

Fig. S7 EDS spectra of (a) C-AuCu nanorods and (b) N-AuCu nanorods.

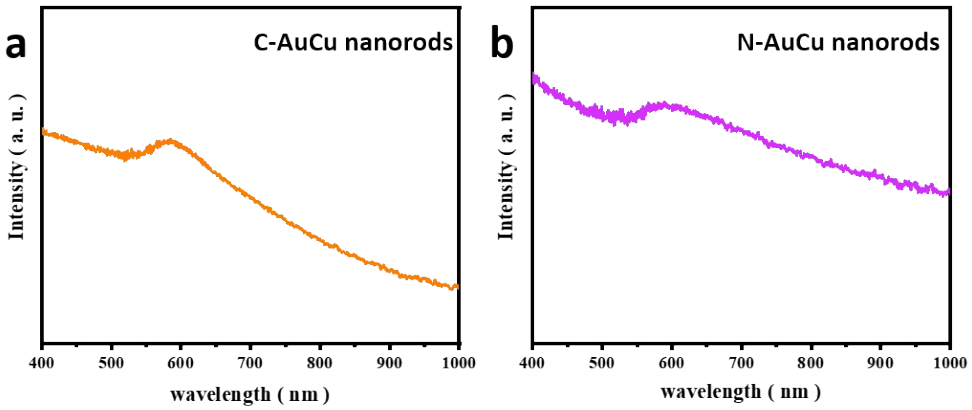

Fig. S8 UV-vis spectra of (a) C-AuCu nanorods and (b) N-AuCu nanorods.

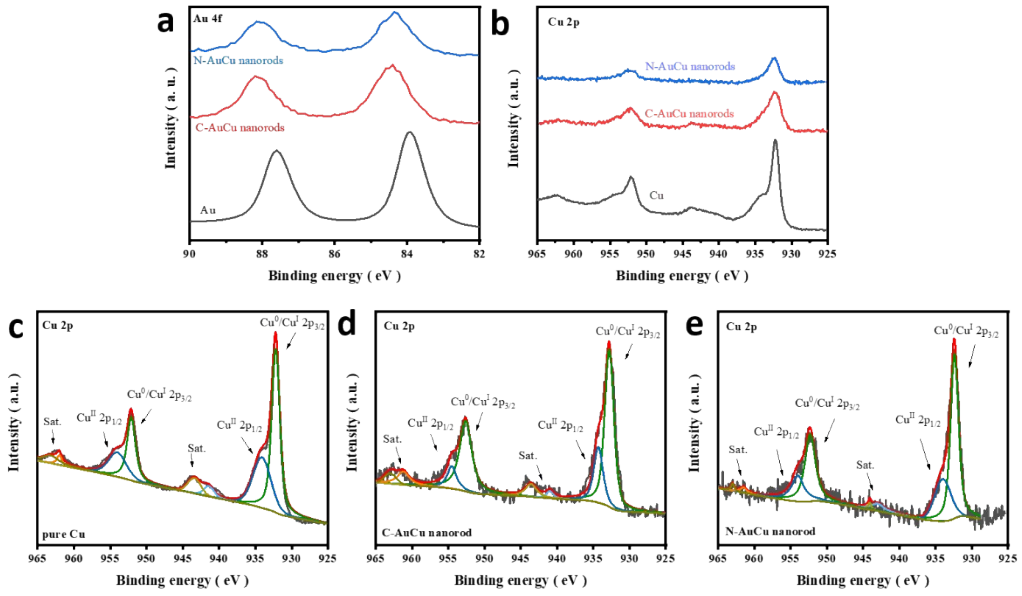

Fig. S9 (a) Au 4f XPS spectra of pure Au nanoparticles, C-AuCu nanorods and N-AuCu nanorods. (b) Cu 2p XPS spectra of pure Cu nanoparticles, C-AuCu nanorods and N-AuCu nanorods. (c-e) Corresponding fitting of Cu 2p XPS spectra for pure Cu nanoparticles, C-AuCu nanorods and N-AuCu nanorods.

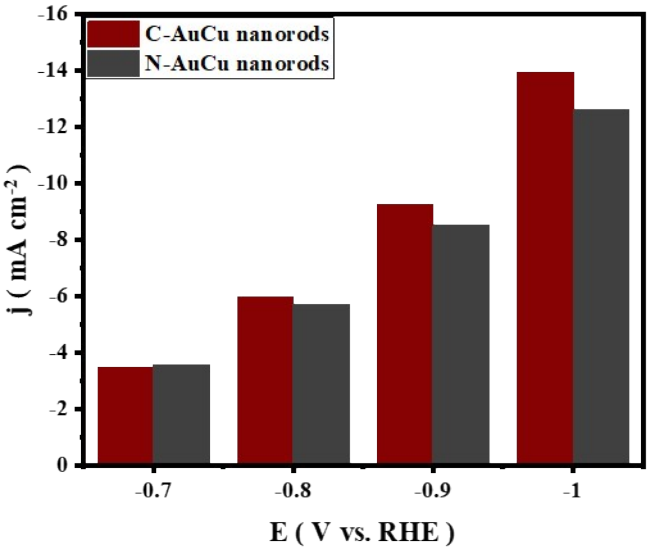

Fig. S10 Current density of C-AuCu nanorods and N-AuCu nanorods under different applied potentials in CO_2RR.

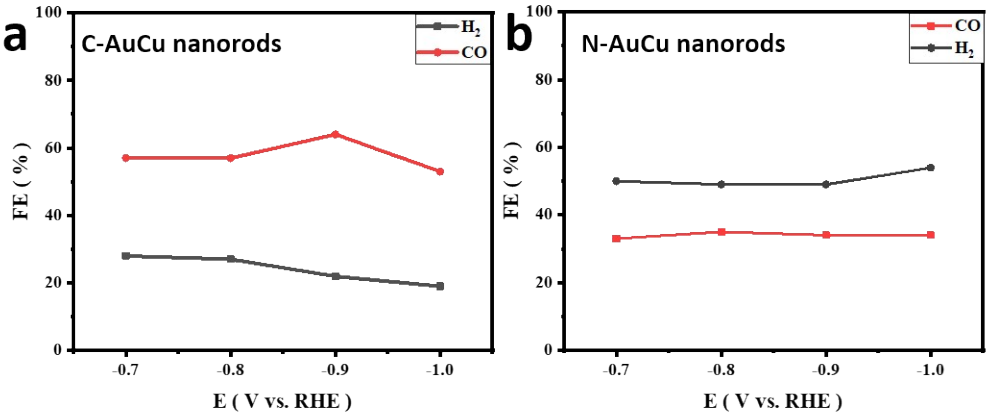

Fig. S11 Faraday efficiencies of CO and H_2 of (a) C-AuCu nanorods and (b) N-AuCu nanorods.